Electrical Resistivity Sounding With an L-Shaped Array

Electrical Resistivity Sounding With an L-Shaped Array

By ADEL A. R. ZOHDY

NEW TECHNIQUES IN DIRECT-CURRENT
RESISTIVITY EXPLORATION

---

*Mathematical criteria and field pro-
cedures for collecting, processing, and
interpreting electrical sounding data
obtained by means of an L-shaped array*

CONTENTS

ILLUSTRATIONS

TABLE

ELECTRICAL RESISTIVITY SOUNDING WITH AN L-SHAPED ARRAY

By Adel A. R. Zohdy

ABSTRACT

The effect of the distant current electrode, B, in the (AMN, B) yL array (L-shaped bipole-dipole perpendicular array) on the value of apparent resistivity is analyzed. A formula is derived for computing the geometric factor of the yL array, and a nomogram is given to simplify computations. A second formula is derived to express the relation between the yL apparent resistivity, $\bar{\rho}_{yL}(AO)$; the ratio of the yL electrode spacings, AO/AB; and the Schlumberger apparent resistivities, $\bar{\rho}_s(AO)$ and $\bar{\rho}_s(BO)$, where AO and BO are the distances from the current electrodes, A and B, to the center, O, of the potential dipole MN. This second formula is used for transforming Schlumberger sounding curves into yL sounding curves. It is also used for determining the limits of the ratio AO/AB, for which a yL sounding curve coincides with a Schlumberger curve. When the resistivity decreases with depth, the ratio AO/AB can be made as large as 0.3 or 0.4 without $\bar{\rho}_{yL}(AO)$ differing from $\bar{\rho}_s(AO)$ by more than 2 percent or 5 percent respectively. When the resistivity increases with depth, the maximum value of the ratio AO/AB should be ≤ 0.15 or ≤ 0.25 for an error of ≤ 2 percent or ≤ 5 percent respectively. Mathematical and field procedures are described for transforming yL sounding curves into Schlumberger curves.

INTRODUCTION

The L-shaped perpendicular array (yL array) is a special electrode configuration of the bipole-dipole perpendicular array (Zohdy, 1970); the measuring dipole MN is placed along a line perpendicular to the current bipole AB at one of the current electrodes A or B (fig. 1). An electrical sounding is made by moving the dipole MN away from the nearest current electrode at logarithmically spaced intervals. At small electrode spacings AO, that is, when $AO \ll AB$, the yL array reduces to the pole-dipole array (or half-Schlumberger array), which is frequently used by some investigators for shallow exploration. However, at large electrode spacings ($AO \gg AB$), the yL array reduces to the perpendicular dipole-dipole array (Al'pin, 1950).

The ideal perpendicular dipole array ($AB \to 0$ and $MN \to 0$) has an intermediate probing depth (Keller, 1966) and an intermediate resolving power (Zagarmistr, 1957) between the ideal equatorial (or azimuthal) and the ideal polar (or radial) dipole-dipole arrays. For example, figure 2
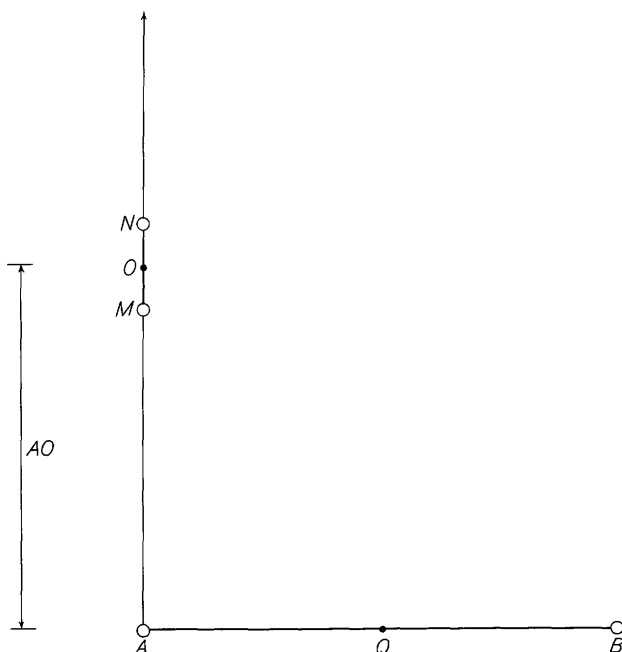
C1

FIGURE 1.—Diagram showing the L-shaped perpendicular array
(*yL* array). *A* and *B*, current electrodes; *M* and *N*, potential
electrodes; *O*, center of dipole *MN*; *Q*, center of bipole *AB*; *AO*,
distance from current electrode to center of dipole.

shows that, for a given three-layer section of the *H* type ($\rho_1 > \rho_2$, $\rho_3 = \infty$),
the ratios of electrode spacings necessary to register the effect of the
electric basement ($\rho_3 = \infty$) are $r_\theta : r_y : r_r = 1 : 1.5 : 2$; but the ordinates of the
apparent resistivities of the minimum points on the respective sounding
curves are $\bar{\rho}_{\theta_{min}} > \bar{\rho}_{y_{min}} > \bar{\rho}_{r_{min}}$. Therefore, the presence of the second
and the third layers is detected on the $\bar{\rho}_\theta$ curve at shorter electrode
spacings than on the $\bar{\rho}_y$ or $\bar{\rho}_r$ curves, which demonstrates the greater
probing depth of the equatorial (or azimuthal) array. However, the effect
of the second layer is most emphasized on the $\bar{\rho}_r$ curve, which demon-
strates the greater resolving power of the polar (or axial) array. The
perpendicular-dipole sounding curve occupies an intermediate position
between the equatorial and the polar curves, which demonstrates its
intermediate probing depth and resolving power.

Bipole-dipole arrays are used more often than dipole-dipole arrays,
and in practice it is impossible to use a true pole-dipole array. It is
important, therefore, to establish the ratios of the electrode spacings at
which a bipole-dipole array approximates either a pole-dipole or a
dipole-dipole array. It is also important to find methods for the interpre-
tation of the data obtained when the dimensions of the electrode array
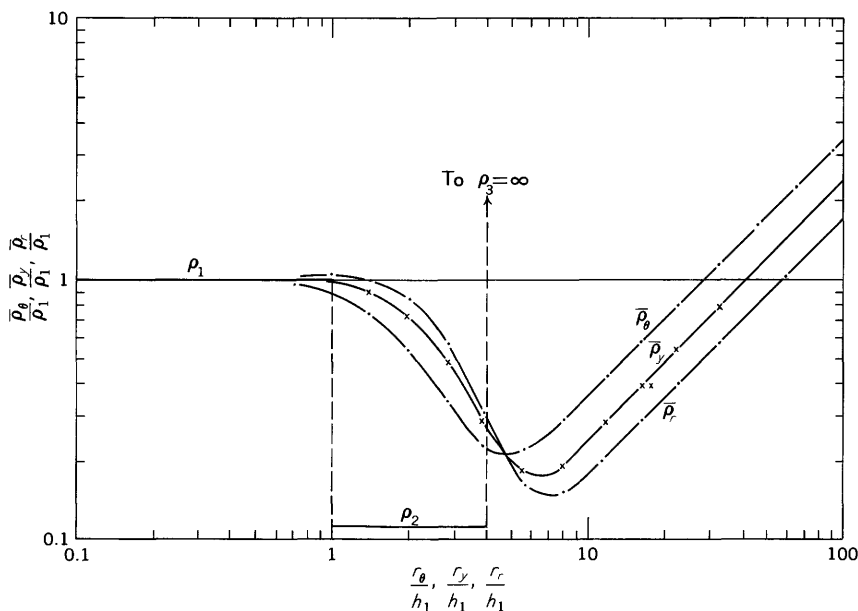do not approximate a pole-dipole or a dipole-dipole array.

FIGURE 2.—Comparison between azimuthal ($\bar{\rho}_\theta$), perpendicular ($\bar{\rho}_y$), and radial ($\bar{\rho}_r$) dipole-dipole three-layer sounding curves for an H-type section ($\rho_2/\rho_1 = \frac{1}{9}$, $\rho_3/\rho_1 = \infty$, $h_2/h_1 = 3$). ρ, true resistivity; $\bar{\rho}$, apparent resistivity; r, dipole spacing; h, thickness of layer.

GEOMETRIC FACTOR OF THE yL ARRAY

The general expression for the geometric factor, K, of a quadripole array is derived from the following expression for the potential difference (Heiland, 1946):

$$\Delta V_{MN}^{A, B} = \frac{\rho I}{2\pi} \left(\frac{1}{AM} - \frac{1}{AN} - \frac{1}{BN} + \frac{1}{BM} \right) = \frac{\rho I}{K}, \tag{1}$$

where ρ is the true resistivity of the medium; AM, AN, BM, and BN are the distances between the electrodes A, M, N, and B; and I is the electric current. For the perpendicular yL array, the geometric factor K in equation 1 may be written as

$$K = \frac{2\pi}{\dfrac{MN}{AM\,AN} - \dfrac{\sqrt{AN^2 + AB^2} - \sqrt{AM^2 + AB^2}}{\sqrt{AM^2 + AB^2}\quad\sqrt{AN^2 + AB^2}}}. \tag{2}$$

When the potential electrode spacing, MN, is small (in comparison to the distance from its center, O, to the nearest current electrode, A, $MN \leqslant 0.1\,AO$), the expression for K is simplified by considering the electric field, E, rather than the potential difference, ΔV. For the bipole-

dipole yL array, the magnitude of the net electric field $E_{yL}^{A,\,B}$ is expressed by

$$E_{yL}^{A,\,B} = E_{AO}^A - E_{BO}^B \cos \alpha, \tag{3}$$

where E_{AO}^A and E_{BO}^B are the magnitudes of the electric fields caused by the point electrodes A and B along the directions AO and BO, respectively, and $\cos \alpha = AO/BO = 1/\sqrt{1 + (AB/AO)^2}$.

For a homogeneous and isotropic half space of resistivity ρ, the magnitudes of the electric fields E_{AO}^A and E_{BO}^B are

$$E_{AO}^A = \frac{\rho I}{2\pi} \frac{1}{AO^2} \tag{4}$$

and

$$E_{BO}^B = \frac{\rho I}{2\pi} \frac{1}{BO^2}. \tag{5}$$

Therefore, substituting equations 4 and 5 in equation 3 and rearranging, we get

$$\rho_{yL}(AO) = \rho = 2\pi AO^2 \left\{ 1 - \frac{1}{\left[1 + \left(\dfrac{AB}{AO} \right)^2 \right]^{3/2}} \right\}^{-1} \frac{E_{yL}^{A,\,B}}{I}, \tag{6}$$

where $\rho_{yL}(AO)$ is the true resistivity, ρ, of the homogeneous and isotropic semi-infinite space as measured by the yL array at the spacing AO. Thus, according to equation 6, the geometric factor for the ideal yL array $(MN \to 0)$ is

$$K_{yL}^\circ = 2\pi AO^2 \left\{ 1 - \frac{1}{\left[1 + \left(\dfrac{AB}{AO} \right)^2 \right]^{3/2}} \right\}^{-1}. \tag{7}$$

In practice, when the distance between the measuring electrodes M and N is finite but nevertheless is sufficiently small (in comparison to the distance from the nearest current electrode), the approximation

$$E_{yL}^{A,\,B} \approx \frac{\Delta V_{MN}^{A,\,B}}{MN} \tag{8}$$

is applicable. Substituting approximation 8 in equation 7 we get

$$\rho_{yL} \approx 2\pi \frac{AO^2}{MN} \left\{ 1 - \frac{1}{\left[1 + \left(\dfrac{AB}{AO} \right)^2 \right]^{3/2}} \right\}^{-1} \frac{\Delta V_{MN}^{A,\,B}}{I}. \tag{9}$$

Therefore the geometric factor for the practical bipole-dipole yL array can be approximated by

$$K_{yL} \approx 2\pi \frac{AO^2}{MN} \left\{ 1 - \frac{1}{\left[1 + \left(\frac{AB}{AO} \right)^2 \right]^{3/2}} \right\}^{-1}. \tag{10}$$

Approximation 10 is simpler than equation 2, and it can be simplified further by expressing K as the product of two factors K_1 and K_2 so that

$$K = K_1 K_2, \tag{11}$$

where

$$K_1 = \frac{AO^2}{MN} \tag{12}$$

and

$$K_2 = 2\pi \left\{ 1 - \frac{1}{\left[1 + \left(\frac{AB}{AO} \right)^2 \right]^{3/2}} \right\}^{-1}. \tag{13}$$

A nomogram for evaluating the factor K_2 for $0.1 \leqslant AO/AB \leqslant 10$ is shown in figure 3. If the distances AO and AB are measured in feet and the resistivity is evaluated in ohm-meters, then the curve denoted by K_2' (where $K_2' = 0.3048 K_2$) should be used. The values of K_2 and K_2' are given in table 1, and an example showing the use of the K_2' curve is given below.

TABLE 1.—*Variation of* K_2 *and* K_2' *as a function of* AO/AB

AO/AB	K_2	K_2'	AO/AB	K_2	K_2'
0.1	6.289	1.917	1.25	11.99	3.652
.125	6.295	1.919	1.666	17.00	5.182
.166	6.311	1.923	2.5	31.48	9.595
.25	6.474	1.943	3.333	51.81	15.79
.333	6.488	1.977	4.0	72.28	22.03
.5	6.900	2.103	5.0	109.9	33.52
.714	7.818	2.382	7.14	218.9	66.74
1	9.72	2.963	10	424.1	129.3

Example.—Let $AB = 500$ feet, $AO = 600$ feet, and $MN = 80$ feet ($MN = 0.133 AO$). Therefore, $K_1 = 36 \times 10^4/80 = 4.5 \times 10^3$ feet; for $AO/AB = 600/500 = 1.2$, the value of K_2' as determined from the nomogram is about 3.5. Therefore the value of the geometric factor is $K_{yL} = K_1 K_2 \approx 1.58 \times 10^4$ meters. The exact value of K_{yL} according to equation 2 is

1.564 × 10⁴ meters, which indicates that the error resulting from the use of the graph in figure 3 is only 1.02 percent. In this example, if $MN \leqslant 0.1 AO$ ($MN \leqslant 60$ feet), the error would be less than 1 percent.
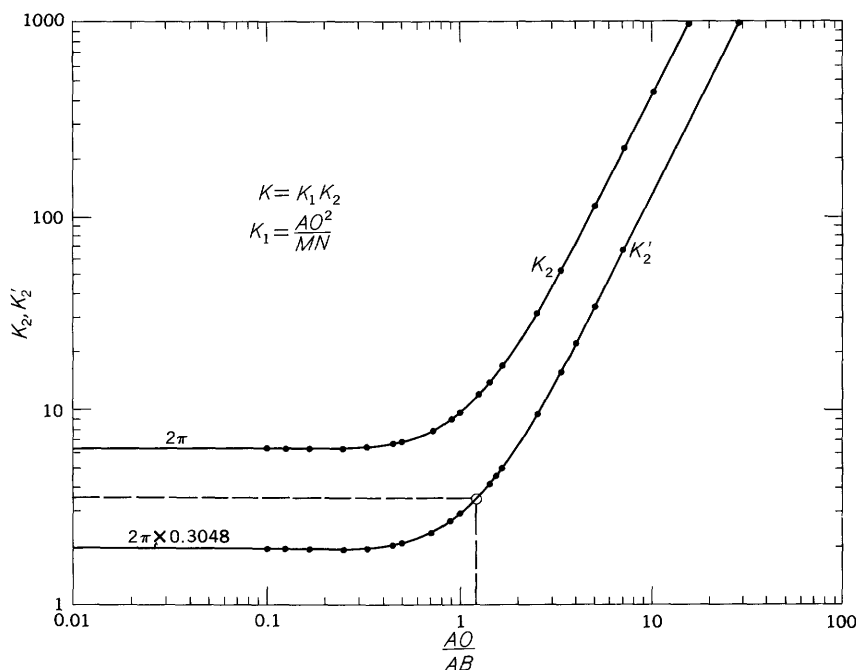

FIGURE 3.—Nomogram for the evaluation of the geometric factor of the yL array. K, geometric factor; AO, distance from current electrode to center of dipole; AB, distance between current electrodes; MN, distance between potential electrodes.

THE yL SOUNDING CURVE

For a horizontally stratified, laterally homogeneous and isotropic medium, the value of the apparent resistivity measured by means of a quadripole array depends not only on the geoelectric parameters of the layers (their thicknesses and resistivities) and on the spacings of the electrode array, but also on the geometry of the array. The dependency on the spacing distances is indicated by considering the rearranged form of equation 1 which (for the computation of the apparent resistivity, $\bar{\rho}$,) is written as

$$\bar{\rho} = 2\pi \left[\frac{1}{AM} - \frac{1}{AN} - \frac{1}{BM} + \frac{1}{AN} \right] \frac{\Delta V_{MN}^{A,B}}{I} \tag{14}$$

In equation 14 the value of $\bar{\rho}$ depends on four variable distances. Consequently, several electrode arrays (Wenner, Schlumberger, and ideal

dipole-dipole arrays) were invented to reduce the dependency of $\bar{p}$ from four distance variables to one distance variable, which in turn reduces the number of theoretical curves necessary for the interpretation of field data.

In yL soundings $(MN \to 0)$, $\bar{p}_{yL}$ depends on the distances AO and BO during the transition from the pole-dipole array $(AO \ll BO)$ to the perpendicular dipole-dipole array $(AO \approx BO)$. The solution to this problem for horizontally stratified, laterally homogeneous media is achieved by one of the following methods:

1. The spacing AO is made much smaller than BO at all times $(AO \leqslant 0.1\ BO)$, and the sounding curves are interpreted by means of the albums of theoretical curves for the Schlumberger array (Compagnie Générale de Géophysique, 1963; Orellana and Mooney, 1966). However, the condition that AO is always less than or equal to 0.1 BO cannot always be fulfilled in practical applications except for very shallow depths of exploration.

2. The ratio AO/BO is held constant for all the sounding measurements. This is done by moving the electrodes MN as well as the current electrode B after each measurement. Then the interpretation of the sounding data is made by calculating special albums of theoretical curves for the designated constant value of AO/BO. A two-layer set of yL sounding curves is shown in figure 4 for the interpretation of data obtained with $AO/BO = \sqrt{2}$ (or $AO/AB = 1$). The calculation of this set was made by using the album of theoretical curves of the Compagnie Générale de Géophysique and by using a formula given in the following section. (See eq 18 and 19.)

RELATION BETWEEN $\bar{p}_{yL}$ AND $\bar{p}_s$

The pattern of the electric field at the surface of a horizontally stratified, laterally homogeneous and isotropic half space, caused by a bipole AB (placed at the surface of the ground), is the same as the pattern obtained over an unstratified homogeneous and isotropic half space. However, the intensity of the electric field at any given point on the horizontally stratified medium is different from the intensity of the field at the same point on the unstratified half space. Therefore, equation 4 for the ideal yL array $(MN \to 0)$ can be applied for a horizontally stratified, laterally homogeneous medium, provided that the electric field E^A and E^B are expressed in terms of the apparent resistivities $\bar{p}_s(AO)$ and $\bar{p}_s(BO)$ of a half-Schlumberger array. Therefore, using equations 3, 4, and 5 we get:

$$E_{AO}^A = \frac{\bar{p}_s(AO)I}{2\pi AO^2},\tag{15}$$

FIGURE 4. — Two-layer master set of γL sounding curves for $AO = AB$. Numbers on curves designate values of ρ_2/ρ_1. A and B, current electrodes; O, center of dipole; ρ, true resistivity; $\bar{\rho}$, apparent resistivity; AO, distance from current electrode to center of dipole; h, thickness of layer.

$$E_{BO}^{B} = \frac{\bar{\rho}_s(BO)I}{2\pi BO^2},$$ (16)

and

$$E_{yL}^{A,B} = \frac{I}{2\pi}\frac{1}{AO^2}\left[\bar{\rho}_s(AO) - \left(\frac{AO}{BO}\right)^3\bar{\rho}_s(BO)\right].$$ (17)

Substituting equation 17 in equation 6, and rearranging we get (Al'pin, 1956):

$$\bar{\rho}_{yL}(AO) = \frac{1}{1-\left(\dfrac{AO}{BO}\right)^3}\left[\bar{\rho}_s(AO) - \left(\frac{AO}{BO}\right)^3\bar{\rho}_s(BO)\right],$$ (18)

or in terms of AO and AB,

$$\bar{\rho}_{yL}(AO) = \frac{1}{1-\left(\dfrac{AO}{\sqrt{AO^2+AB^2}}\right)^3}\left[\bar{\rho}_s(AO) - \left(\frac{AO}{\sqrt{AO^2+AB^2}}\right)^3\bar{\rho}_s(BO)\right].$$

(19)

Equations 18 and 19 are used to transform theoretical Schlumberger curves (Compagnie Générale de Géophysique, 1963; Orellana and Mooney, 1966) into yL sounding curves. However, because theoretical Schlumberger curves are expressed in terms of the dimensionless quantities AO/h_1 and $\bar{\rho}_s/\rho_1$ (where ρ_1 and h_1 are the unit resistivity and unit thickness of the first layer), equation 19 may be written in the dimensionless form

$$\frac{\bar{\rho}_{yL}(AO/h_1)}{\rho_1} = \frac{1}{1-\left[\dfrac{AO/h_1}{\sqrt{(AO/h_1)^2+(AB/h_1)^2}}\right]^3}$$

$$\times\left[\frac{\bar{\rho}_s(AO/h_1)}{\rho_1} - \left(\frac{AO/h_1}{\sqrt{(AO/h_1)^2+(AB/h_1)^2}}\right)^3\frac{\bar{\rho}_s(BO/h_1)}{\rho_1}\right].$$

The calculated values of the reduced resistivity $\bar{\rho}_{yL}(AO/h_1)/\rho_1$ may be plotted as a function of the reduced spacing AO/h_1, but the resulting yL sounding curve will also depend on the value of AB/h_1. To illustrate this dependency, a set of yL sounding curves was computed for a two-layer earth model in which the second layer is a perfect insulator ($\rho_2=\infty$).
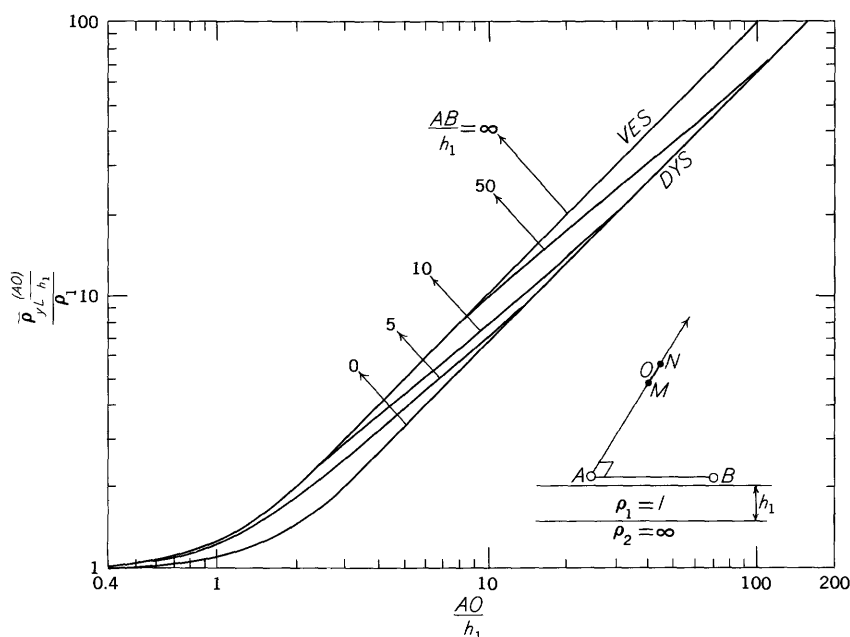
FIGURE 5.—Two-layer yL sounding curves obtained over a buried insulator ($\rho_2 = \infty$) for variable AO/AB. ρ, true resistivity; $\bar{\rho}$, apparent resistivity; AO, distance from current electrode to center of dipole; A and B, current electrodes; M and N, potential electrodes; O, center of dipole; h_1, thickness of first layer. VES, half-Schlumberger, or pole-dipole curve; DYS, dipole-dipole perpendicular curve.

The set shown in figure 5 is composed of five curves corresponding to $AB/h_1 \to \infty$ (half-Schlumberger, pole-dipole, or VES curve), $AB/h_1 = 50$, 10, 5, and $AB/h_1 \to 0$ (dipole-dipole perpendicular, or DYS, curve).

Considering the set of curves shown in figure 5, the following conclusions are drawn for yL sounding curves obtained over a two-layer structure with $\rho_2 = \infty$, $AB =$ constant, and $AO =$ variable:

1. An infinite number of theoretical yL sounding curves is obtained as a result of the infinite number of values that the ratio AB/h_1 may attain. A single curve, however, is obtained if $AO/AB =$ constant.
2. A yL sounding curve ($AB =$ constant) coincides with the pole-dipole (Schlumberger) curve as $AB/h_1 \to \infty$, and coincides with the ideal dipole-dipole perpendicular sounding (DYS) curve as $AB/h_1 \to 0$.
3. The general form of a two-layer yL sounding curve ($\rho_2 = \infty$), obtained with $AB/h_1 =$ constant, resembles a three-layer Schlumberger curve of the A type (Kalenov, 1957; Keller and Frischknecht, 1966) or the sounding curve obtained by a symmetric $AMNB$ Schlumberger array over a two-layer medium with a buried vertical step fault (Faradzhev, 1958a, b; Kunetz, 1966).

4. In order to obtain a sufficiently long segment of a two-layer yL sounding curve (AB = constant) that can be interpreted by means of a two-layer Schlumberger curve, the distance between the current electrodes must be at least 20 times the depth to the buried insulator ($AB/h_1 \geqslant 20$). Larger AB/H ratios generally would be required for multilayer earth models, where H is the total depth to the electric basement, because of the possible effect of pseudoanisotropy (Zohdy, 1965) owing to the presence of resistive layers within the section.

5. The two-layer yL sounding curve ($\rho_2 = \infty$) deviates from the corresponding VES curve at $AO/AB \approx 0.2$ and merges with the corresponding DYS curve at $AO/AB \approx 4$. Therefore, if the ratio $AO/AB \leqslant 0.2$, then the data can be interpreted using theoretical VES curves. This, however, does not necessarily mean that the obtained curve segment (at $AO/AB \leqslant 0.2$) would be of sufficient length to justify a dependable interpretation (as, for example, when $AB/h_1 \leqslant 10$).

6. For different values of AB/h_1, the general form of the yL sounding curve remains unchanged from where it deviates from the rectilinear right branch of the Schlumberger curve (S-line) to where it merges with the rectilinear rising branch of perpendicular dipole-dipole curve.

The mathematical proof for conclusion 6 is as follows. Equation 18 is rewritten as

$$\bar{\rho}_{yL}(AO) = \frac{\bar{\rho}_s(AO)}{1 - \left(\dfrac{AO}{BO}\right)^3} \left[1 - \left(\frac{AO}{BO}\right)^2 \frac{\bar{\rho}_s(BO)}{BO} \frac{AO}{\bar{\rho}_s(AO)} \right],$$

but for $\bar{\rho}_s$ values on the S-line,

$$\frac{\bar{\rho}_s(BO)}{BO} = \frac{1}{S} \text{ and } \frac{AO}{\bar{\rho}_s(AO)} = S,$$

where S is the total longitudinal conductance (Kalenov, 1957; Keller and Frischknecht, 1966). Therefore, on the S-line,

$$\frac{\bar{\rho}_s(AO)}{\bar{\rho}_{yL}(AO)} = \frac{1 - \left(\dfrac{AO}{BO}\right)^3}{1 - \left(\dfrac{AO}{BO}\right)^2} \tag{20}$$

Equation 20 indicates that the ratio $\bar{\rho}_s(AO)/\bar{\rho}_{yL}(AO)$, which is an index of the deviation of the yL sounding curve from the Schlumberger sounding curve, along the S-line, is a function only of the ratio AO/BO.
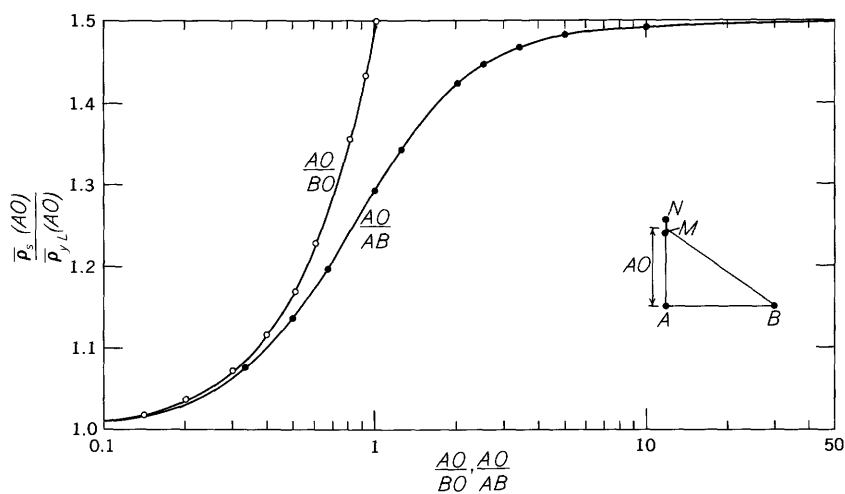
FIGURE 6.—Variation of the effective resistivity factor $\bar{\rho}_s(AO)/\bar{\rho}_{yL}(AO)$ as a function of the spacing ratios AO/BO and AO/AB. $\bar{\rho}$, apparent resistivity; AO and BO, distances between current electrodes and center of dipole; AB, distance between current electrodes; M and N, potential electrodes.

The ratio $\bar{\rho}_{yL}(AO)/\bar{\rho}_s(AO)$ may be called the "effective resistivity factor." In equation 20 when $BO \gg AO$ (pole-dipole array), $\bar{\rho}_s(AO)/\bar{\rho}_{yL}(AO) = 1$, and when $BO \approx AO$ (perpendicular dipole-dipole array), $\bar{\rho}_s(AO)/\bar{\rho}_{yL}(AO) = 3/2$; this is proved by applying l'Hospital's rule (Wylie, 1951) to equation 20.

In figure 6, the variation of the effective resistivity factor $\bar{\rho}_s(AO)/\bar{\rho}_{yL}(AO)$ as a function of AO/BO is shown as the curve having open circles, and its variation as a function of AO/AB is shown as the curve having solid circles. These curves are useful in constructing the S-line of the Schlumberger curve from data obtained by the yL array, provided that the effect of a high-resistivity electric basement is detected on the yL sounding curve. The procedure for this construction is as follows: (1) Calculate the value of AO/AB, (2) determine from the solid-circle curve in figure 6 the value of the ordinate $\bar{\rho}_s(AO)/\bar{\rho}_{yL}(AO)$, (3) multiply the measured value of $\bar{\rho}_{yL}(AO)$ by the ratio $\bar{\rho}_s(AO)/\bar{\rho}_{yL}(AO)$ to determine $\bar{\rho}_s(AO)$ and (4) plot the value of $\bar{\rho}_s(AO)$ at the spacing value AO.

It should be emphasized that the transformation procedure using the effective resistivity factor $\bar{\rho}_s(AO)/\bar{\rho}_{yL}(AO)$ is strictly applicable to apparent resistivity values that correspond to the detection of a high-resistivity electric basement ($\rho_{\text{bedrock}} \to \infty$) and that it does not accurately transform all the data on the yL sounding curve into a Schlumberger sounding curve. This limitation also applies to the transformation of sounding data using the so-called effective spacing factor as defined by Keller (1966).

As mentioned earlier, when the ratio $AO/AB \leq 0.2$, the two-layer yL sounding curve for $\rho_2 \to \infty$ does not depart considerably from the pole-dipole (half Schlumberger) curve. When $\rho_2 \neq \infty$, the limiting value of the ratio AO/AB, for which a pole-dipole curve is obtained, depends on the geoelectric parameters of the section. For example, it is obvious that, when sounding measurements are made over a homogeneous and isotropic half space, the true resistivity of the medium is determined correctly irrespective of the value of AO/AB (provided that the exact value of the geometric factor is used in the calculation). Therefore, to study the effect of the distant current electrode B and the error introduced in the results when that effect is neglected, we write equation 18 in the following form:

$$\bar{\rho}_{yL}(AO) = \bar{\rho}_s(AO) \left[\frac{1}{1 - \left(\dfrac{AO}{BO}\right)^3} - \frac{(AO/BO)^3}{1 - (AO/BO)^3} \frac{\bar{\rho}_s(BO)}{\bar{\rho}_s(AO)} \right].$$

Adding 1 and subtracting 1 in the term in the brackets and rearranging, we get

$$\frac{\bar{\rho}_{yL}(AO)}{\bar{\rho}_s(AO)} = 1 + \frac{(AO/BO)^3}{1 - (AO/BO)^3} \left[1 - \frac{\bar{\rho}_s(BO)}{\bar{\rho}_s(AO)} \right].$$

The second term in the preceding equation is the disturbing factor that makes the ratio $\bar{\rho}_{yL}(AO)/\bar{\rho}_s(AO)$ different from unity. Therefore, by setting this second term to be equal to or less than 0.05 or 0.02, respectively, or by setting

$$\frac{(AO/BO)^3}{1 - (AO/BO)^3} \left[1 - \frac{\bar{\rho}_s(BO)}{\bar{\rho}_s(AO)} \right] \leq \pm 0.05 \qquad (21)$$

and

$$\frac{(AO/BO)^3}{1 - (AO/BO)^3} \left[1 - \frac{\bar{\rho}_s(BO)}{\bar{\rho}_s(AO)} \right] \leq \pm 0.02, \qquad (21')$$

we determine the limiting conditions for the values of $\bar{\rho}_{yL}(AO)$ to be equal to $\bar{\rho}_s(AO)$ with an error of ± 5 percent, or ± 2 percent, respectively.

For a 5-percent error we rearrange equation 20 and, in terms of AO and AB, write it in the forms

$$\frac{AO}{AB} \leq \frac{1}{\sqrt{\left[20 \dfrac{\bar{\rho}_s(BO)}{\bar{\rho}_s(AO)} - 19 \right]^{2/3} - 1}}, \text{ for } \frac{\bar{\rho}_s(BO)}{\bar{\rho}_s(AO)} \geq 1, \qquad (22)$$

and

$$\frac{AO}{AB} \leq \frac{1}{\sqrt{\left[21 - 20 \dfrac{\bar{\rho}_s(BO)}{\bar{\rho}_s(AO)} \right]^{2/3} - 1}}, \text{ for } \frac{\bar{\rho}_s(BO)}{\bar{\rho}_s(AO)} \leq 1. \qquad (23)$$
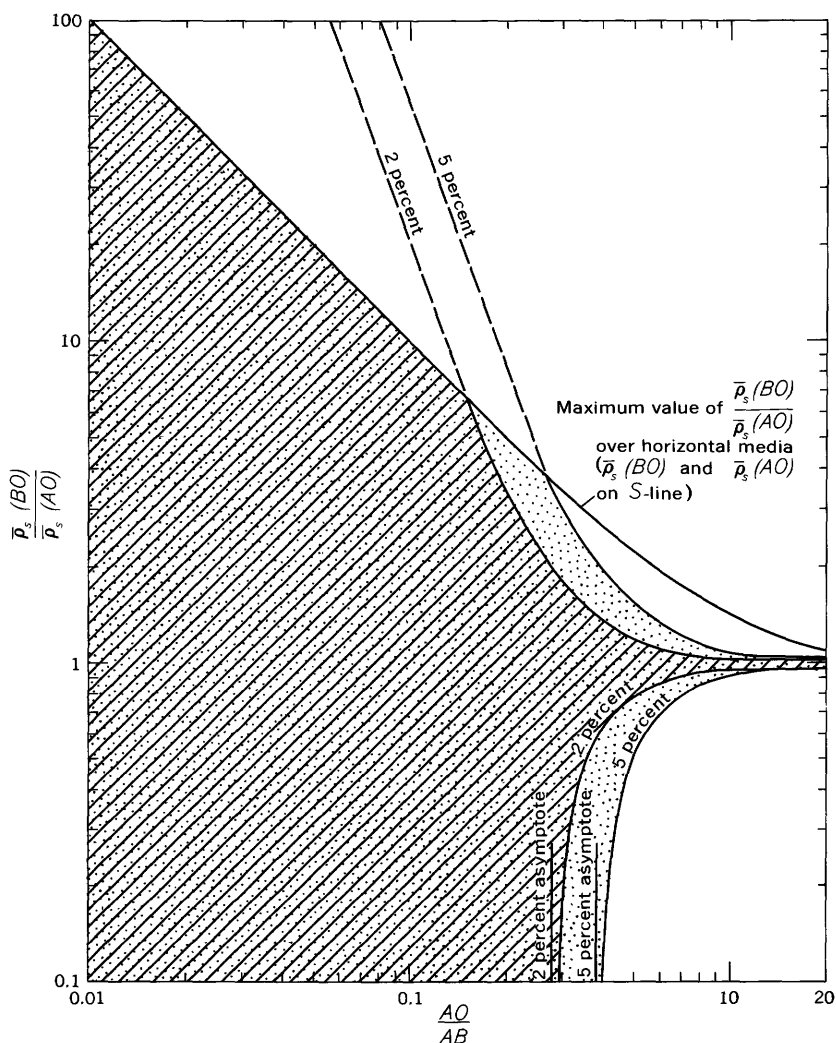
FIGURE 7. — Variation of $\bar{\rho}_s(BO)/\bar{\rho}_s(AO)$ as a function of AO/AB for an error in $\bar{\rho}_{yL}(AO)$ of 2 percent and 5 percent. Hatched area results in errors in $\bar{\rho}_{yL}(AO)$ of less than 2 percent; stippled area, in errors in $\bar{\rho}_{yL}(AO)$ of less than 5 percent. $\bar{\rho}$, apparent resistivity; AO and BO, distances between current electrodes and center of dipole; AB, distance between current electrodes; S-line, rectilinear branch of a VES curve rising at an angle of 45° with the abscissa axis.

Similar expressions are found for evaluating a 2-percent error using equation 21'. The variation of $\bar{\rho}_s(BO)/\bar{\rho}_s(AO)$ as a function of AO/AB for errors in $\bar{\rho}_{yL}(AO)/\bar{\rho}_s(AO)$ of ± 5 percent and ± 2 percent are shown in figure 7. A curve for the maximum values of $\bar{\rho}_s(BO)/\bar{\rho}_s(AO)$, which are

obtained when both $\bar{\rho}_s(BO)$ and $\bar{\rho}_s(AO)$ fall on the S-line, is also shown in figure 7. The curves in figure 7 indicate that, when $\bar{\rho}_s(BO) \ll \bar{\rho}_s(AO)$ (steeply descending branch on a Schlumberger curve), the ratio AO/BO may be made as large as approximately 0.3 without introducing an error greater than 2 percent, or it may be made as large as approximately 0.4 without introducing an error greater than 5 percent. For a moderately descending branch the ratio AO/BO can be made larger than 0.3, or 0.4, respectively. When $\bar{\rho}_s(BO) \gg \bar{\rho}_s(AO)$, the ratio of AO/AB should be made equal to or smaller than 0.15 for a 2-percent error or less, or it should be made equal to or smaller than 0.26 for a 5-percent error or less.

In practice, the exact value of $\bar{\rho}_s(BO)$ is not known beforehand, but if the general form of the sounding curve in the area can be anticipated from other data, then the proper "safe" ratio AO/AB can be estimated from the curves in figure 7. A similar analysis for horizontal profiling using the pole-dipole and the polar dipole-dipole array was made by Russian investigators (Blokh, 1957 and 1962; Blokh and Shemyakin, 1959), who seemed to disregard the fact that this type of analysis applies only to horizontally stratified media and not to media with inclined or vertical contacts (unless the electric fields created by images placed across the contact are considered).

COLLECTING AND PROCESSING OF yL SOUNDING DATA

Several methods were outlined by Al'pin (1956) for the transformation of electrical sounding data obtained by the so-called asymmetric or angular soundings. The method for processing yL sounding data will closely follow Al'pin's derivations.

Equation 18 can be rearranged in the form

$$\bar{\rho}_s(AO) = \left[1 - \left(\frac{AO}{BO} \right)^3 \right] \bar{\rho}_{yL}(AO) + \left(\frac{AO}{BO} \right)^3 \bar{\rho}_s(BO). \qquad (18')$$

The values of AO/BO and $\bar{\rho}_{yL}(AO)$ are measured in the field, but in order to calculate the Schlumberger apparent resistivity $\bar{\rho}_s(AO)$ from 18' the value of the second Schlumberger resistivity $\bar{\rho}_s(BO)$ at the spacing BO must be determined, especially when AO/AB is large. The value of $\bar{\rho}_s(BO)$ cannot be determined independently from $\bar{\rho}_s(AO)$ unless the effect of the current electrode A is eliminated. Therefore, in the field, by orienting the potential line MN at right angles to the line AO, we eliminate the contribution of the current electrode A, and we make a measurement of the apparent resistivity $\bar{\rho}_{xL}$ with the L-shaped parallel bipole-dipole array (xL array).
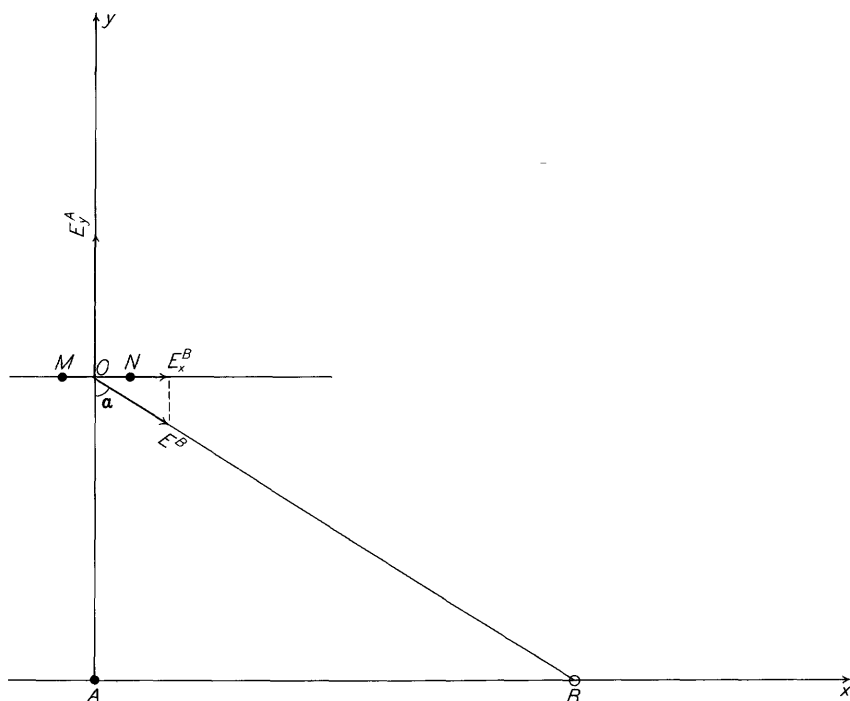
FIGURE 8.—The L-shaped parallel array (xL array). A and B, current electrodes; M and N, potential electrodes; O, center of dipole; E^B, electric field at O caused by point source at B; E_x^B, horizontal component of the electric field E^B; E_y^A, electric field at O caused by point source at A.

Considering figure 8, the horizontal component of the electric field, E_x^B, is related to the total field E^B (caused by the point source at B) by

$$E_x^B = E^B \sin \alpha,$$

or

$$E^B = E_x^B \frac{BO}{AB}. \tag{24}$$

For a homogeneous and isotropic semi-infinite space, the true resistivity ρ is calculated from

$$\rho = 2\pi BO^2 \frac{E^B}{I}. \tag{25}$$

In the xL array, the horizontal component E_x^B, rather than the field E^B, is measured. Therefore, substituting equation 24 in equation 25 we get

$$\rho = 2\pi \frac{BO^3}{AB} \frac{E_x^B}{I} \tag{26}$$

For a horizontally stratified, laterally homogeneous medium the apparent resistivity is substituted for the true resistivity, and we therefore write equation 26 as

$$\bar{\rho}_{xL} = 2\pi \frac{BO^3}{AB} \frac{E_x^B}{I} = \bar{\rho}_s(BO), \tag{27}$$

where $\bar{\rho}_{xL}$ is the apparent resistivity measured by means of the xL array and is calculated by measuring the electric field

$$E_x^B \approx \frac{\Delta V_{MN}^B}{MN}. \tag{28}$$

Therefore, substituting approximation 28 in equation 27 we get

$$\rho_{xL} \approx \frac{2\pi}{MN} \frac{BO^3}{AB} \frac{\Delta V_{MN}^B}{I},$$

or

$$\bar{\rho}_{xL} \approx 2\pi \frac{(AO^2 + AB^2)^{3/2}}{AB \cdot MN} \frac{\Delta V_{MN}^B}{I}. \tag{29}$$

The exact value of $\bar{\rho}_{xL}$ may also be calculated from the exact but more complicated expression

$$\bar{\rho}_{xL} = 2\pi \frac{\sqrt{\left(AB + \frac{MN}{2}\right)^2 + AO^2} \sqrt{\left(AB + \frac{MN}{2}\right)^2 + AO^2}}{\sqrt{\left(AB + \frac{MN}{2}\right)^2 + AO^2} - \sqrt{\left(AB - \frac{MN}{2}\right)^2 + AO^2}} \frac{\Delta V_{MN}^B}{I}. \tag{30}$$

When $MN \leq 0.1AO$, the value of $\bar{\rho}_{xL}$ as determined from equation 30 differs from its value as determined from approximation 29 by less than 1 percent.

Substituting the measured value of $\bar{\rho}_{xL}$ for $\bar{\rho}_s(BO)$ in equation 18′, and having measured $\bar{\rho}_{yL}$ and substituting it in equation 18′ also, the value of $\bar{\rho}_s(AO)$ is calculated. The Schlumberger curve $\bar{\rho}_s(AO) = f(AO)$ is thus obtained by making two apparent resistivity measurements, $\bar{\rho}_{yL}$ and $\bar{\rho}_{xL}$. Furthermore, the value of $\bar{\rho}_{xL}(BO) = \bar{\rho}_s(BO)$ (used in the calculation of $\bar{\rho}_s(AO)$) can be plotted as part of the Schlumberger curve at the spacing BO. Therefore, in effect, the two measurements $\bar{\rho}_{yL}(AO)$ and $\bar{\rho}_{xL}(BO)$ are used to obtain two Schlumberger resistivities, $\bar{\rho}_s(AO)$ (by calculation, using eq. 18′ on p. C15) and $\bar{\rho}_s(BO) = \bar{\rho}_{xL}(BO)$ (by observation).

If we utilize the above procedure in practice, we realize that, as the

spacing AO is increased, the spacing $BO = \sqrt{AO^2 + AB^2}$ is increased at a much smaller rate, especially for $0.2 < AO/AB < 2$. For example, if $AB = 10$ length units, then for $AO/AB < 0.2$, $\bar{\rho}_{yL}(AO) \approx \bar{\rho}_s(AO)$, and there is no need to measure $\bar{\rho}_{xL}(BO) \approx \bar{\rho}_s(BO)$. Then at $AO = 2.5$ length units, $BO = 10.29$ length units, and a measurement of $\bar{\rho}_{xL}(BO) = \bar{\rho}_s(BO)$ is made to calculate $\bar{\rho}_s(AO)$ (from eq. 18'), to plot $\bar{\rho}_s(AO)$ at $AO = 2.5$ length units, and to plot $\bar{\rho}_{xL}(BO)$ at $AO = 10.29$ length units. Then, as measurements of $\bar{\rho}_{yL}(AO)$ are made at $AO = 3, 4, 5, 6,$ and 8 length units (which corresponds to an increasing logarithmic increment of 1.2 to 1.3), the value of BO ranges from 10.29 length units (at $AO = 2.5$) to 12.8 length units (at $AO = 8$). This means that as AO changes through a logarithmic interval of $8/3 = 2.66$, BO changes through a logarithmic interval of about 1.24 only. Therefore, it is sufficient to make only two measurements of $\bar{\rho}_{xL}(BO)$, one at $AO/AB = 0.25$ and the other at $AO/AB = 0.8$. The values of $\bar{\rho}_{xL}(BO)$ for $0.25 < AO/AB < 0.8$ that are necessary for the calculation of $\bar{\rho}_s(AO)$ at $AO = 3, 4, 5,$ and 6 length units are easily obtained by interpolation between the values of $\bar{\rho}_{xL}(BO)$ at $BO = 10.29$ and $\bar{\rho}_{xL}(BO)$ at $BO = 12.8$, which would be sufficiently close if the data are obtained over a horizontally homogeneous medium.

The following AO/AB values are recommended for making measurements of $\bar{\rho}_{xL}(BO)$: $AO/AB = 0.25, 0.8, 1.2, 1.6,$ and 2.0. For values of $AO/AB \geq 2$ the azimuth angle $\theta = \angle AQO$, where Q is the center of AB, is greater than or equal to 76°. It is difficult to measure $\bar{\rho}_{yL}(AO)$ at $\theta > 75°$ because $K_{yL} \to \infty$ as $\theta \to 90°$. Furthermore, for $AO/AB \geq 2.5$, $AO \approx BO$, and it is of little use to measure $\bar{\rho}_s(AO)$ and $\bar{\rho}_s(BO)$ when the spacings AO and BO are separated by a very small logarithmic interval. Therefore, for $AO/AB \geq 2.5$, it is sufficient to measure $\bar{\rho}_{xL}(BO)$ only and to plot it at the electrode spacing value of $BO = \sqrt{AO^2 + AB^2}$.

SUMMARY AND CONCLUSIONS

Electrical soundings using L-shaped electrode arrays can be made either with the ratio of the electrode spacings AO/AB held constant or with AO/AB held variable and AB held constant. When the ratio AO/AB is held constant, the sounding curves are interpreted using sets of theoretical curves that are based on the given constant value of AO/AB. Such sets are easily derived from the available albums of Schlumberger theoretical curves. When AO/AB is variable and AB is held constant, yL sounding data are almost identical to Schlumberger sounding data for most resistivity contrasts, provided that $AO/AB < 0.2$. When $0.2 \leq AO/AB \leq 2$, the yL sounding data must be complemented by measurements with the parallel L-shaped array (xL array) in order to calculate the equivalent Schlumberger apparent resistivity. Only three or four resistivity measurements, made by the xL array, are necessary

for the entire range of $0.2 \leqslant AO/AB \leqslant 2$, and for $AO/AB > 2$ it is sufficient to measure the value of $\bar{\rho}_{xL}(BO)$, which is equal to the Schlumberger resistivity $\bar{\rho}_s(BO)$.

Electrical sounding with an L-shaped array with AO variable and AB held constant is very useful in obtaining subsurface information at great depths in areas where road networks make it difficult to make all the required symmetric $AMNB$ Schlumberger soundings. Moreover, for each setup of the current electrodes A and B, the potential electrodes can be moved along four lines perpendicular to the line AB at the electrodes A and B. Consequently a great amount of detailed study can be made with a minimum movement of the current electrodes.

REFERENCES CITED

Al'pin, L. M., 1950, [The theory of dipole sounding]: Moscow, Gostoptekhizdat, 88 p. (in Russian); English translation in Keller, G. V., 1966, Dipole methods for measuring earth conductivity, New York, Consultants Bur., p. 1–60.
——— 1956, [The asymmetrical (angular) sounding]: Prikladnaya Geofizika, v. 14, p. 65–96 (in Russian).
Blokh, I. M., 1957, [Dipole electroprofiling]: Moscow, Gosgeoltekhizdat, 190 p. (in Russian).
——— 1962, [The resistivity method of electroprofiling]: Moscow, Gosgeoltekhizdat, 238 p. (in Russian).
Blokh, I. M., and Shemyakin, E. A., 1959, [Construction of dipole and three electrode electroprofiling charts from investigations of straight-line unsymmetric BAMN systems]: Akad. Nauk SSSR Izv. Ser. Geof. 70.6, p. 872–879 (in Russian); English translation by J. J. Loferski, 1960, Bulletin (Izvestiya), no. 6, p. 614–619.
Compagnie Générale de Géophysique, 1963, Master curves for electrical soundings: The Hague, European Assoc. Explor. Geophysicists.
Faradzhev, A. S., 1958a, [Model studies of electrical soundings over a screen and a step]: Razved. i Promyslovaya Geofizika, v. 23, p. 38–44 (in Russian).
——— 1958b, [A study of the effect of non-horizontal boundaries on the results of electrical soundings]: Prikladnaya Geofizika, v. 19, p. 109–128 (in Russian); English translation by Ivan Mittin, 1966, in U.S. Geol. Survey library, Denver, 36 p.
Heiland, C. A., 1940, Geophysical exploration: New York, Prentice-Hall, Inc., 1013 p.
Kalenov, E. N., 1957, [Interpretation of vertical electrical sounding curves]: Moscow, Gostoptekhizdat, 471 p. (in Russian).
Keller, G. V., 1966, Dipole method for deep resistivity studies: Geophysics, v. 31, p. 1088–1104.
Keller, G. V., and Frischknecht, F. C., 1966, Electrical methods in geophysical prospecting: Pergamon Press, 517 p.
Kunetz, Géza, 1966, Principles of direct current resistivity prospecting: Berlin-Nikolassee, Gebrüder Borntraeger, 103 p.
Orellana, Ernesto, and Mooney, H. M., 1966, Master tables and curves for vertical electrical sounding over layered structures: Madrid, Interciencia, 34 p., 125 tables, and supplement of theoretical curves. (In English and Spanish.)
Wylie, C. R., Jr., 1951, Advanced engineering mathematics [1st ed.]: New York, McGraw-Hill Book Co., Inc., 696 p.
Zagarmistr, A. M., 1957, [Utilization of the increased resolving power of dipole-axial soundings in investigating a "type-H" section]: Prikladnaya Geofizika, v. 16, p.

130–144 (in Russian); English translation by Ivan Mittin, 1966, in U.S. Geol. Survey library, Denver, 21 p.

Zohdy, A. A. R., 1965, The auxiliary point method of electrical sounding interpretation and its relationship to the Dar Zarrouk parameters: Geophysics, v. 30, no. 4, p. 644–660.

——1970, Geometric factors of bipole-dipole arrays: U.S. Geol. Survey Bull. 1313–B, 26 p.